IL-1β, TNF-α and TGFβ1 regulate mouse amelotin gene transcription in

gingival epithelial cells

（IL-1β、TNF-α および TGFβ1 は歯肉上皮細胞においてマウスアメロ

チン遺伝子の転写を調節する）

日本大学大学院松戸歯学研究科歯学専攻

能田　佳祐

（指導:　小方　頼昌　教授）

Preface

This article is based on a main reference paper, "IL-1β and TNF-α regulate mouse amelotin gene transcription in gingival epithelial cells" in the Journal of Oral Science, and a reference paper, "TGFβ1-induced Amelotin gene expression is downregulated by Bax expression in mouse gingival epithelial cells" in the Journal of Oral Science.

Abstract

Amelotin (AMTN) is an enamel protein expressed in maturation stage ameloblasts and junctional epithelium. In the first study, to elucidate the transcriptional regulation of AMTN gene by interleukin-1β (IL-1β) and tumor necrosis factor-α (TNF-α), we conducted real-time PCR, Western blotting, transient transfection analyses with luciferase constructs including the various length of mouse AMTN gene promoter, gel shift and chromatin immunoprecipitation assays using mouse gingival epithelial GE1 cells. AMTN mRNA and protein levels were increased after 6 h stimulation by IL-1β (1 ng/ml) and TNF-α (10 ng/ml) in GE1 cells. IL-1β and TNF-α induced luciferase activities of the constructs between -116$AMTN$ to -800$AMTN$ of mouse AMTN gene promoter. Transcriptional activation by IL-1β and TNF-α were partially inhibited by 3-bp mutations inserted in the CCAAT-enhancer-binding protein 1 (C/EBP1), C/EBP2

and Yin Yang 1 (YY1) elements in the -460*AMTN*. Transcriptional activities induced by IL-1β and TNF-α were inhibited by tyrosine kinase, MEK1/2 and PI3-kinase inhibitors. Results of ChIP assays showed that IL-1β and TNF-α increased C/EBPβ and YY1 binding to C/EBP1, C/EBP2 and YY1 elements.

In the second study, we investigated the transcriptional downregulation of TGFβ1-induced AMTN gene expression in GE1 cells in a progressed apoptosis phase. To examine the effects of TGFβ1 on AMTN, Smad3 and Bax mRNA levels in mouse gingival epithelial GE1 cells, real-time PCR analyses were performed. And then, transient transfection analyses were completed using the several lengths of mouse AMTN gene promoter constructs including Smad response elements with or without TGFβ1. Overexpression of Bax dramatically downregulated TGFβ1-induced AMTN mRNA levels and transcriptional activities of AMTN gene.

In conclusion, in the first study, we demonstrated that IL-1β and TNF-α increased AMTN gene transcription via C/EBP1, C/EBP2 and YY1 elements in the mouse AMTN gene promoter. In the second study, we showed that TGFβ1-induced AMTN mRNA levels were downregulated by Bax overexpression in the mouse gingival epithelium cells. These results suggest that AMTN could be involved in the defense mechanism of periodontal tissue.

Introduction

Junctional epithelium (JE) is composed of confluence of the oral epithelium and the reduced enamel epithelium during teeth eruption. JE is located on the internal part of the marginal gingiva with its firmly attachment to the enamel surface (1). JE cells exhibit rapid turnover, which contributes to the host-parasite equilibrium and rapid repair of gingival damage such as inflammation and trauma (2).

Amelotin (AMTN) is a secreted enamel protein, expressed by maturation stage ameloblasts and internal basal lamina of JE. Localization of AMTN suggests its function as an adhesin for JE cells to the tooth surface (3-7). AMTN expressed in the JE at the erupted molars of mice similar to odontogenic ameloblast-associated protein (ODAM) (5). AMTN transgenic mice under the amelogenin gene promoter have thinner and irregular enamel (6). AMTN-deficient mice revealed hypomineralized inner enamel and structure defects in the outer enamel due to the delayed kallikrein-4 expression (8). During JE regeneration following gingivectomy, ODAM was expressed first at the leading wound edge and AMTN appeared later, suggesting ODAM and AMTN have a task at the cell-tooth interface (9). AMTN can promote hydroxyapatite mineralization (10).

4

Chronic periodontitis is an inflammatory disease caused by periodontopathic bacteria and viruses. That will cause alveolar bone resorption, gum swelling, bleeding, tooth mobility, occasional pain and tooth loss (11, 12). The immune response to bacteria and its produced substances, such as lipopolysaccharide (LPS) and proteolytic enzymes, and succeeding production of inflammatory cytokines and other inflammatory mediators, play an important role in destruction of periodontium (13, 14). Interleukin-1β (IL-1β) is a notable inflammatory mediator responsive to cell proliferation, differentiation, apoptosis, and in the pathophysiology of periodontal disease (15). IL-1β concentrations in the gingival crevicular fluid could reflect severity of symptoms associated with periodontal disease and the values indicate inflammation levels more sensitive than clinical parameters of periodontal disease such as probing pocket depth and bleeding on probing as markers of gingival inflammation (16). Tumor necrosis factor-α (TNF-α) is an important cytokine of both acute and chronic inflammatory responses in many diseases, such as postmenopausal osteoporosis, rheumatoid arthritis (RA), and periodontitis (17).

Several of proapoptotic factors which translocate to the outer mitochondrial membrane and oligomerizes following its activation, such as Bim (18), Bik (19) and Bax (20), play a dependent role in important regulatory step in promoting apoptosis in

gingival epithelium by making the membrane permeable to cytochrome c (21). Some reports showed relationship between apoptosis and periodontitis. For example, *Aggregatibacter actinomycetemcomitans* which highly detected in periodontal pockets with aggressive periodontitis induces apoptosis of gingival epithelium cells associated with phosphorylation of Smad2 and inhibition of Bcl2 (22, 23).

We have previously demonstrated that AMTN gene expression significantly increased in inflamed gingiva (24, 25). AMTN gene expression is temporarily increased at the initiation of apoptosis induced by transforming growth factor beta1 (TGF-β1) via Smad3 signaling pathways in gingival epithelium in gingival epithelial cells (26). These reports suggest AMTN might play a critical role in development and maintaining homeostasis of JE. However, there is no report of regulation AMTN gene transcription by inflammatory cytokines in the gingival epithelial cells. In this study, we have analyzed the effects of IL-1β and TNF-α on the expression of AMTN gene in mouse gingival epithelial cells. Furthermore, to present evidence that TGFβ1-induced AMTN gene expression was inhibited during the progression of apoptosis in mouse gingival epithelial cells, we examined that overexpression of Bax influences the change of AMTN gene expression.

Materials and Methods

Reagents

Alpha-minimum essential medium (α-MEM), IL-1β, TNF-α and Apoptosis *in situ* Detection Kit were purchased from Wako (Tokyo, Japan). SFM-101 was purchased from Nissui (Tokyo, Japan). Recombinant Human Transforming growth factor β1 (TGFβ1) were purchased from R&D Systems, Inc. (240-B-010, Minneapolis, MN, USA). Fetal calf serum (FCS), Lipofectamine 2000, penicillin and streptomycin, and TrypLE Express were purchased from Invitrogen (Carlsbad, CA, USA). pGL3-basic luciferase plasmid, pSV-β-galactosidase (β-Gal) control plasmid, mitogen-activated protein kinase kinase (MAPKK or MEK1/2) inhibitor U0126 and pCMV5 control vector were obtained from Promega (Madison, WI, USA). The protein kinase A (PKA) inhibitor KT5720, the tyrosine kinase inhibitor herbimycin A (HA), phenylmethylsulfonyl fluoride (PMSF, serine protease inhibitor) and BAX Inhibiting Peptide V5 (BIPV5; B1436) were purchased from Sigma-Aldrich Japan (Tokyo, Japan). The PKC inhibitor H7 was obtained from Seikagaku Corporation (Tokyo, Japan), and the phosphatidylinositol 3-kinase (PI3K) inhibitor LY249002 was purchased from Calbiochem (San Diego, CA, USA). Smad3 (MGC Mouse Smad3 cDNA, clone Id: 30432720) and pCMV-SPORT6.0 Bax (MGC Mouse Bax cDNA, clone Id: 6489475)

were purchased from Thermo Fisher Scientific Biosciences Corp. (Lafayette, USA and Kanagawa, Japan). The PrimeScript RT reagent kit and SYBR Premix Ex Taq™ II were obtained from Takara-bio (Tokyo, Japan). Protein A agarose/Salmon sperm DNA was purchased from Millipore (Temecula, CA, USA). ELC plus Western Blotting Detection Reagents and Hybond 0.2 μm PVDF membrane were purchased from GE Healthcare (Pittsburgh, PA, USA). Quikchange Site-directed Mutagenesis Kit was obtained from Stratagene (La Jolla, CA, USA). All chemicals used were of analytical grade.

Cell culture

Mouse gingival epithelial GE1 cell (RCB1709) was purchased from RIKEN BRC (Ibaraki, Japan), and cultured at 33 °C in 5% CO_2 and 95% air in α-MEM or SFM-101 containing 1% FCS, 10 ng/ml EGF, 1% penicillin and streptomycin. Cells were grown to confluence in 60 mm culture dishes, then cultured for 12 h in α-MEM or SFM-101 without FCS, and stimulated with IL-1β (1 ng/ml), TNF-α (10 ng/ml) or TGFβ1 (10 ng/ml) . Total RNA was purified from triplicate cultures at 3, 6, 12, and 24 h after stimulation and analyzed for genes that were stimulated by IL-1β and TNF-α. Then GE1 cells were incubated in SFM-101 with or without TGFβ1 (10 ng/ml) by time dependent or for 24 h. Bax and Smad3 expression vectors at concentration of 2, 4 and 6 μg/ml in

the medium were used dose dependent overexpression of Bax (pCMV-SPORT6.0 Bax) and Smad3 (pCMV-SPORT6.0 Smad3). Forty-eight hours after plating to 60 mm dishes, cells at approximately 50-70% confluence were transfected using a lipofectamine 2000. pCMV5 vector was used as a control.

Real-time polymerase chain reaction (PCR)

Total RNA (1 μg) was used as a template for cDNA synthesis. cDNA was prepared using the PrimeScript RT reagent kit. Quantitative real-time PCR was performed using the SYBR Premix Ex Taq II in a TP800 thermal cycler dice real-time system (Takara-Bio, Tokyo, Japan) and the following primer sets: mouse AMTN For; 5'-CTGTCAACCAGGGAACCACT-3'; mouse AMTN Rev; 5'-TGTGATGCGGTTTAGCTGAG-3', mouse Smad3 For; 5'-AGGGGCTCCCTCACGTTATC-3'; mouse Smad3 Rev; 5'-CATGGCCCGTAATTCATGGTG-3', mouse Bax For; 5'-CCGGCGAATTGGAGATGAACTG-3'; mouse Bax Rev; 5'-AGCTGCCACCCGGAAGAAGACCT-3' and mouse glyceraldehyde-3-phosphate dehydrogenase (GAPDH) For; 5'- AAATGGTGAAGGTCGGTGTG-3'; mouse GAPDH Rev; 5'-TGAAGGGGTCGTTGATGG-3'. The PCR reactions were performed in a total

volume of 25 μl, 2x SYBR Premix Ex Taq II (12.5 μl), 10 μM forward and reverse primers and 50 ng cDNA for AMTN and 10 ng cDNA for GAPDH. PCR premixes containing all reagents except for cDNA were prepared and aliquoted into 0.2 mL PCR tubes. The conditions for thermal cycling were 10 s at 95°C, and 40 cycles of 5 s at 95°C and 30 s at 60°C. Post-PCR melting curves confirmed the specificity of single-target amplification, and the expression of AMTN relative to GAPDH was determined in triplicate.

Western blotting

For the Western blotting, cell lysates of GE1 cells were separated in 12% sodium dodecyl sulfate (SDS)-polyacrylamide gel electrophoresis (SDS-PAGE) and transferred to a PVDF membrane. The membrane was then incubated for 3 h with anti-amelotin polyclonal antibody (ab122312; Abcam, Cambridge, UK), anti-Bax (1:1000; ab7977, Abcam), anti-Smad3 (1:3000; ab28379, Abcam), anti-phosphorylated Smad3 (pSmad3, phospho S423 + S425, 1:2000; ab52903, Abcam), anti-cdk2 (1:1000; sc163, Santa Cruz Biotechnology), anti-β-Actin antibodies (1:1000; sc1616, Santa Cruz biotechnology). and anti-α tubulin monoclonal antibody (sc-5286; Santa Cruz Biotechnology, Paso Robles, CA, USA). Peroxidase conjugated anti-rabbit and mouse IgG antibodies

(Sigma-Aldrich, St. Louis, MO, USA) and anti-goat IgG (1:5000; HRP-conjugate, 12-348, Millipore) antibodies were used as the secondary antibodies. Immunoreactivities were detected using ECL plus Western Blotting Detection Reagents.

Luciferase assays

To study the IL-1β and TNF-α response regions in the mouse AMTN gene promoter, we prepared chimeric constructs by ligating mouse AMTN gene promoters into luciferase reporter plasmid. Different lengths of mouse AMTN gene promoter fragments (-116*AMTN*; -116~+60, -238*AMTN*; -238~+60, -460*AMTN*; -460~+60, -705*AMTN*; -705~+60, -800*AMTN*; -800~+60) were prepared by PCR amplification. These promoter DNAs were cloned into the Sac I site of the pGL-3basic multi-cloning site. Mutation luciferase constructs, mutation CCAAT enhancer binding protein 1 (mC/EBP1), mutation C/EBP2 (mC/EBP2), double mutations in C/EBP1 and C/EBP2 (mC/EBP1+mC/EBP2) and mutation Ying Yang 1 (mYY1) were made using the Quikchange Site-directed Mutagenesis Kit within the context of the homologous -460*AMTN* promoter fragments. All constructs were sequenced as described previously to verify the fidelity of the mutagenesis.

Gingival epithelial GE1 cells were used for transient transfection assays. Twenty-four

hours after plating, cells at 60-70% confluence were transfected using Lipofectamine 2000. The transfection mixture included 1 μg of the respective luciferase (LUC) construct and 2 μg β-Gal vector as an internal control. β-Gal activities were determined separately to normalize the values. Two days after transfection, the cells were cultured in α-MEM without FCS for 12 h, and then stimulated with 1 ng/ml IL-1β or 10 ng/ml TNF-α for 12 h prior to harvest. The luciferase activities were measured in accordance with the supplier's protocol using a luminescence reader (AcuuFlex Lumi 400; Aloka, Tokyo, Japan). The PKC inhibitor H7 (5 μM), PKA inhibitor KT5702 (100 nM), tyrosine kinase inhibitor HA (1 μM), MEK1/2 inhibitor U0126 (5 μM) and PI3K inhibitor LY249002 (10 μM) were used for protein kinase inhibitors. GE1 cells were also used for transfection assays using TGFβ1 (10 ng/ml). The transfection mixture included 2 μg of the respective LUC construct (-1651$AMTN$, -1651~+65), 1 μg β-Gal vector as an internal control, pCMV5 vector or Bax overexpression plasmid (6 μg/60 mm dish). Two days after transfection, cells were deprived of FCS and EGF for 12 h, and TGFβ1 (10 ng/ml) in no-serum SFM-101 media (10 ng/ml) were added for 24 h prior to harvesting.

Gel shift assays

Confluent GE1 cells stimulated by IL-1β (1 ng/ml) or TNF-α (10 ng/ml) for 0, 3, 6 and

12 h in α-MEM without FCS were used to prepare the nuclear extracts. Double-stranded

oligonucleotides encompassing the 5'-Cy5-labeled C/EBP1, C/EBP2 and YY1

sequences in the mouse AMTN promoter were prepared. Nuclear proteins (3 μg) were

incubated for 20 min at room temperature (RT) with 2 pM Cy5-labeled double-stranded

oligonucleotide in buffer containing 50 mM KCl, 0.5 mM EDTA, 10 mM Tris-HCl (pH

7.9), 1 mM dithiothreitol, 0.04% Nonidet P-40, 5% glycerol and 1 μg of poly(dI/dC).

After incubation, the DNA-protein complexes were separated by electrophoresis in 6%

non-denaturing acrylamide gels run at 200 V at RT. After electrophoresis, the gels were

scanned using a Typhoon TRIO+ Variable Mode Imager (GE Healthcare). For

competition experiments, 40-fold molar unlabeled oligonucleotides of C/EBP1, C/EBP2

and YY1 were used. The double-stranded oligonucleotide sequences were: C/EBP1 (nts.

-117 to -108, For; 5'-CCCTAATGAAGTGTTGGGAAATGAAACCA-3', Rev;

5'-GGATTACTTCACAACCCTTTACTTTGGGT-3'); C/EBP2 (nts. -163 to -151, For;

5'-CCTCGTAGACATTGGGTAATACAATGTCA-3',   Rev;

5'-GAGCATCTGTAACCCATTATGTTACAGT-3') and YY1 (nts. -228 to -212, For;

5'-CCTTTTCTGTCTGTCTGCACTTTTTTAAAATTA-3',   Rev;

5'-GAAAAGACAGACGTGAAAAAATTTTAAT-3').

Chromatin immunoprecipitation (ChIP) assays

To determine the interaction between specific transcription factors and DNA *in vivo* in the mouse AMTN gene promoter, ChIP assays were performed using GE1 cells. Confluent GE1 cells in 100 mm culture dishes were stimulated by IL-1β (1 ng/ml) or TNF-α (10 ng/ml) for 0, 6, 12, and 24 h, and then the cells were fixed with 160 μl formaldehyde for 10 min to crosslinking the DNA-protein complexes. The fixed cells were rinsed two times by a wash buffer [1 mM phenylmethylsulfonyl fluoride (PMSF) and complete protease inhibitor cocktail (Sigma-Aldrich) in the PBS (-)] on ice, collected by scraper and centrifuged for 5 min at 4 °C. After the cells were resuspended by a SDS buffer (1% SDS, 0.01 M EDTA, 0.05 M Tris-HCl, pH 8.1), lysates were sonicated to shear the DNA-protein complexes. Sonicated cell supernatants were diluted in a 10-fold ChIP buffer (0.01% SDS, 1.1% Triton X-100, 1.2 μM EDTA, 16.7 mM Tris-HCl, pH8.9, 16.7 mM NaCl, 1 mM PMSF and complete protease inhibitor cocktail). The diluted supernatants were assigned Input as a control which included non-specific DNA-protein complexes, and pre-cleared with 80 μl salmon sperm DNA/Protein A-agarose (50% Slurry) for 30 min at 4 °C with gentle agitation. For the immunoprecipitation of DNA-protein complexes, 2 μg of appropriate antibody [C/EBPβ

(△198; sc-746; Santa Cruz Biotechnology) and anti-YY1 antibody (ab38422; abcam)] were used for 100 µl of precleared supernatant, incubated overnight at 4 °C with constant rotation. Sixty µl of salmon sperm DNA/Protein A-agarose (50% Slurry) was added for 1 h at 4 °C with rotation to collect the antibody/histone complexes and pellet agarose by gentle centrifugation (1,000 rpm for 1 min). After removing the supernatant that contained unbound chromatin, the pellet was washed with 1 ml each of Low Salt buffer (0.1% SDS, 1% Triton X-100, 2 mM EDTA, 20 mM Tris-HCl, pH 8.1, 150 mM NaCl), High Salt buffer (0.1% SDS, 1% Triton X-100, 2 mM EDTA, 20 mM Tris-HCl, pH 8.1, 500 mM NaCl), LiCl buffer (0.25 M LiCl, 0.1% NP-40, 1% deoxycholate, 0.5 mM EDTA, 0.01 M Tris-HCl, pH 8.1), and 1 ml of TE buffer (10 mM Tris-HCl, pH 8.1, 1 mM EDTA) twice. After the TE buffer was removed, Protein A-agarose/antibody/chromatin complexes were resuspended in a 250 µl elution buffer (1% SDS and 0.1 M NaHCO3) and incubated at RT for 15 min with gentle rotation. After the spin down of the agarose beads, 20 µl 5 M NaCl was added to the supernatant for reverse cross-links, and 10 µl 0.5 M EDTA, 20 µl 1 M Tris-HCl, pH 6.5, and 1 µl 10 mg/ml proteinase K were added to the degradate of the antibodies and proteins. DNA was recovered by phenol/chloroform/isoamylalcohol extraction and ethanol precipitation. The purified DNA was subjected to PCR amplification (1 cycle of 3 min

at 95°C, 35 cycles of 15 s at 95°C, 15 s at 55 or 56°C, 1 min at 72°C, and 1 cycle of 1

min at 72°C) for the C/EBP1, C/EBP2 and YY1 sites within the mouse AMTN

promoter using C/EBP1 For, 5'-CAATGTCTGCAGCTAATAAC-3'; C/EBP1 Rev,

5'-GACAGACAACCTGAGAGACC-3';   C/EBP2   For,

AAAATTATATAGGCATGTCTCCC-3';   C/EBP2   Rev,

TTCATTAGGAGGGTTATTAGC-3';   YY1   For,

5'-GCAAAAGAGTTGAAAGTAAAG-3';   YY1   Rev,

CTACGATCTGACTAGAGGGT-3'; primer. KAPA Taq™ Extra HotStart was utilized

for the PCR analyses. Furthermore, to investigate whether Bax overexpression

abrogated the Smad3 specific bindings to Smad binding elements (SBEs) *in vivo* in the

mouse AMTN gene promoter, ChIP assays were performed in GE1 cells. Bax (2 or 6

μg) overexpression plasmids were transfected by using a lipofectamine 2000 into

approximately 50-70% confluent GE1 cells. pCMV5 vector was used as a control. Two

μg of the rabbit polyclonal anti-Smad3 antibody (ab28379, Abcam) and the appropriate

unconjugated normal rabbit anti-IgG antibody (sc-2027, Santa Cruz, Inc.) were used for

the immunoprecipitation of protein-DNA complexes per one sample.

Apoptosis analysis

To evaluate the apoptosis *in situ* by Bax overexpression, TUNEL staining was carried

out using an Apoptosis *in situ* Detection Kit (Wako, Osaka, Japan). GE1 cells were

plated on culture slides (Falcon® CultureSlides, Corning® BioCoat™) and transfected

Bax expression vector (2, 4 and 6 μg/ml) in SFM-101 media. Two days post transfection,

cells were deprived of serum for 24 h. The cells were fixed by 4% paraformaldehyde

(PFA) for 10 min at RT, prior to following the procedure in accordance with the

manufacturer's protocol.

Statistical analysis

In each experiment, triplicate samples were analyzed and experiments were replicated to

ensure the consistency of the responses to the cytokines. Significant differences between

the control and treatment groups were determined using the one-way ANOVA.

Results

Effects of IL-1β or TNF-α on mouse AMTN mRNA and protein levels in GE1 cells

To investigate the effects of IL-1β or TNF-α on AMTN transcription, we used GE1 cells

which express AMTN mRNA constitutively. At first, the dose-response effects of IL-1β

and TNF-α on the AMTN mRNA levels were evaluated by treating the cells with

different concentrations of IL-1β or TNF-α for 12 h. IL-1β increased AMTN mRNA

levels maximal at 1 and 10 ng/ml (Fig. 1A). TNF-α induced AMTN mRNA levels

maximal at 10 and 50 ng/ml (Fig. 1C). Treatment of GE1 cells with IL-1β (1 ng/ml)

increased AMTN mRNA levels at 6 h, reached maximum at 12 and 24 h (Fig. 1B).

TNF-α (10 ng/ml) up-regulated AMTN mRNA levels at 6 h, and reached maximum at

12 and 24 h (Fig. 1D). IL-1β (1 ng/ml) and TNF-α (10 ng/ml) increased AMTN protein

expressions at 6 h and reached them maximum at 12 and 24 h (Fig. 2).

Luciferase analyses of mouse AMTN gene promoter constructs

To elucidate the site of IL-1β and TNF-α regulated transcription in the 5'-flanking

region of the mouse AMTN gene, various-sized promoter DNAs ligated to a luciferase

plasmid were transiently transfected into GE1 cells and their transcriptional activities

were measured in the presence or absence of IL-1β or TNF-α. The luciferase activity of

-116*AMTN*, which encompasses nucleotides from -116 to +60, was increased after 12 h

treatment with IL-1β (1 ng/ml) or TNF-α (10 ng/ml) in GE1 cells (Fig. 3). IL-1β and

TNF-α also up-regulated the luciferase activities of -238*AMTN* (-238~+60), -460*AMTN*

(-460~+60), -705*AMTN* (-705~+60) and -800*AMTN* (-800~+60) (Fig. 3). Within the

DNA sequence that is unique in the AMTN gene promoter, an inverted CCAAT box

(ATTGG; nts -66 to -62), a Sex-determining region Y (SRY, AAACCAA; nts -99 to -93), a C/EBP1 (GTGTTGGGAAA; nts -112 to -102), an Oct-1 (CTCCTAATGAAGT; nts -123 to -111), a C/EBP2 (ACATTGGGTAATA; nts -157 to -144) and a YY1 (TGTCTGCACTTTTT; nts -221 to -207) elements (Fig. 4). Next, we introduced 3-bp mutations within the -460*AMTN* constructs in the C/EBP1, C/EBP2 and YY1 elements. Transcriptional inductions by IL-1β and TNF-α were partially inhibited by 3-bp mutations inserted in the C/EBP1, C/EBP2 and YY1, and almost completely inhibited by double mutations in the C/EBP1 and C/EBP2 (Fig. 5). IL-1β and TNF-α-induced luciferase activities (-460*AMTN*) were inhibited by HA, U0126 and LY294002, but not inhibited by H7 and KT5720, suggesting involvement of tyrosine kinase, MEK1/2 and PI3K in the signaling pathways (Fig. 6).

Gel mobility shift assays

To determine nuclear proteins that bind to the C/EBP1, C/EBP2 and YY1, and mediate IL-1β and TNF-α effects on transcription, Cy5 labeled double-stranded oligonucleotides were incubated with nuclear proteins (3 μg) extracted from GE1 cells that were either not treated (Control) or treated with IL-1β (1 ng/ml) or TNF-α (10 ng/ml) for 3, 6, and 12 h. Using nuclear extract from confluent GE1 cells without stimulation (Control),

shifts of C/EBP1-, C/EBP2- and YY1-protein complexes were evident (Fig. 7A and B,

lanes 1, 5 and 9). After stimulation by IL-1β (1 ng/ml) or TNF-α (10 ng/ml),

C/EBP1-protein complexes were increased at 12 h (Fig. 7A and B, lane 4).

C/EBP2-protein complexes were increased at 3 h, which retain the same condition until

12 h (Fig. 7A and B, lanes 6, 7 and 8). YY1-protein complex were increased at 6 and 12

h (Fig. 7A and B, lanes 11 and 12). Specificity of DNA-protein complexes were

confirmed by competition gel shifts in a 40-fold molar excess of non-labeled C/EBP1,

C/EBP2 and YY1 to reduce DNA-protein complex formations (Fig. 8A and B, lanes 3, 7

and 11). Whereas the C/EBP2 did not compete with YY1-protein complex formations

(Fig. 8A and B, lane 12), C/EBP2 and C/EBP1 partially competed with the C/EBP1 and

C/EBP2-protein complex formations (Fig. 8A and B, lanes 4 and 8).

ChIP assays

ChIP assays were performed to clarify whether transcription factors are able to interact

directly with the mouse AMTN gene promoter and how IL-1β and TNF-α influence the

interactions of these transcription factors with C/EBP1, C/EBP2 and YY1 elements in

the GE1 cells. C/EBPβ binding to C/EBP1 was increased by IL-1β and TNF-α at 12 h,

and decreased at 24 h. L-1β and TNF-α increased C/EBPβ binding to C/EBP2 at 3 h,

reached maximum at 12 h, and decreased at 24 h. YY1 binding to YY1 element was increased by IL-1β at 12 h, and decreased at 24 h. TNF-α increased YY1 binding to YY1 element at 6 h and reached maximum at 12 and 24 h (Fig. 9A and B). Next we investigated which signaling pathways can regulate C/EBPβ and YY1 bindings to C/EBP1, C/EBP2 and YY1 after stimulation with IL-1β and TNF-α, KT5720 (PKA inhibitor), HA (tyrosine kinase inhibitor), U0126 (MEK1/2 inhibitor) and LY294002 (PI3K inhibitor) were used with or without IL-1β or TNF-α treatment. When GE1 cells were stimulated with IL-1β or TNF-α for 12h, C/EBPβ and YY1 binding to C/EBP1, C/EBP2 and YY1 elements were almost completely inhibited by HA, U0126 and LY294002. However, KT5720 could not (Fig. 10A and B).

Effects of TGFβ1 on mouse AMTN, Smad3 and Bax mRNA and AMTN protein levels in GE1 cells

We showed that TGFβ1-induced AMTN gene expression was gradually reduced in time dependent course. AMTN mRNA levels were temporally increased at 24 h treatment of TGFβ1 (10 ng/ml), and gradually decreased at 48 and 72 h treatment of TGFβ1 (Fig. 11A). Similarly, AMTN expression were increased by TGFβ1 (10 ng/ml) and reached at maximal levels by 48 h treatment of TGFβ1, then greatly reduced at 72 h. Actin

expression were not changed as controls (Fig. 11B). Smad3 and Bax mRNA levels were increased by TGFβ1 (10 ng/ml) time dependently, and continue to be induced at least at 72 h treatment of TGFβ1 (Fig. 11C, D).

Overexpression of Bax influences the change of AMTN gene expression.

Dose dependent overexpression of Bax induced apoptosis of GE1 cells, positive cells by TUNEL staining were detected mainly at overexpression of Bax (4 and 6 μg) (Fig. 12A). The apoptosis induced by Bax overexpression (6 μg) were represented by positive detection in GE1 cells in the absence of BIPV5 peptide, and Bax-mediated cell death in GE1 cells was slightly decreased by incubation with BIPV5 peptide (200 μM) for 72 h. In the presence of higher concentrations of BIPV5 peptide, the apoptotic cells by Bax overexpression were hardly detected. These results suggested that Bax overexpression was specifically induced apoptosis without cytotoxicity in GE1 cells (Fig. 12B). We next investigated if Bax expression suppresses AMTN mRNA levels induced by TGFβ1. Treatment of TGFβ1 (10 ng/ml) for 24 h upregulated AMTN mRNA levels. Transfection of Bax inhibited the TGFβ1-induced AMTN mRNA levels in dose-dependent manner (Fig.13A). The transcriptional activities of the AMTN promoter constructs, -1651*AMTN* (-1651~+65) including SBEs, were increased by TGFβ1 (10

ng/ml) for 24 h in agreement with previous study. Overexpression of Bax (6 μg) abrogated the basal and TGFβ1-induced transcriptional activities of AMTN gene promoter (Fig.13B). These results suggested that Bax overexpression silenced the TGFβ1-induced transcriptional upregulation of AMTN gene.

The mechanism that TGFβ1-upregulated AMTN mRNA levels were prevented by Bax overexpression

Smad3 expression in nuclear and cytosol were increased by treatment of TGFβ1 for 24 h, and Smad3 expression in nuclear were also slightly increased by overexpression of Bax (2 and 6 μg) in dose dependent (Fig. 14A). Phosphorylated Smad3 (pSmad3) expression were also increased by treatment of TGFβ1 for 24 h, and Bax overexpression did not influence to phosphorylation of Smad3. While, Bax expression was not detected in nuclear. TGFβ1-induced Smad3 and Bax expression in cytosol were slightly upregulated in the presence of Bax overexpression, compared with those in absence of Bax overexpression. These findings could imply that Bax expression was not involved in directly down-regulation of Smad3 expression and the phosphorylation of Smad3 in nuclear. On the contrary, Bax expression induced Smad3 protein expression levels in nuclear and cytosol, although Bax reduced the effect of TGFβ1-stimulation on the

upregulation of Smad3 and Bax. (Fig. 14A). We suspected that the overexpression of

Bax blocked Smad3 bindings to SBEs in the AMTN gene promoter without reduction of

Smad3 expression in nuclear. Smad3 bindings to the SBEs, which including SBE3-8,

were upregulated by TGFβ1 (10 ng/ml) treatment and reached maximal at 24 h.

Overexpression of 2 μg/ml Bax did not affect the Smad3 binding to the SBEs, however

overexpression of 6 μg/ml Bax completely inhibited Smad3 bindings to the SBEs (Fig.

14B).

Discussion

In the first study, we have shown that IL-1β and TNF-α increased AMTN gene

transcription in gingival epithelial GE1 cells targeting C/EBP1, C/EBP2 and YY1

elements in the mouse AMTN gene promoter. IL-1β and TNF-α increased C/EBPβ

binding to C/EBP1 and C/EBP2 elements, and YY1 binds to YY1 element in the

proximal promoter of the mouse AMTN gene. Various cells produce cytokines which

are strong local mediators of inflammation. IL-1β and TNF-α are major cytokines that

play a large role in the periodontal inflammation process (27). IL-1β and LPS induced

macrophage inflammatory protein-1α (MIP-1α) which is a cysteine-cysteine chemokine

in gingival epithelial cells. In the inflamed periodontium, MIP-1α positive cells are

more abundant than other chemokine-positive cells and the expression is increased in a

number of diseases characterized by inflammation induced bone loss (28). TNF-α,

TNF receptor type 1 (TNFR1) and receptor activator of nuclear factor kappa-B (NF-κB)

ligand (RANKL) were coexpressed in JE. TNF-α induced RANKL expression mediated

through TNFR1 and PKA signaling pathways (29). Ohno *et al.* reported a novel cascade

comprising sequential LPS, angiopoietin-like protein 2, integrin α5β1 and inflammatory

cytokine induction which could be responsible for inducing periodontal disorganization

in gingival epithelial cells (30). C/EBPβ and NF-κB are involved in the regulation of

gene expressions which fill the role in inflammation, immunity and malignant processes

(31). Inflammatory lipid sphingosine-1-phosphate increases C-reactive protein via

C/EBPβ and promotes breast cancer progression (32). C/EBPβ is implicated in

inflammatory lung disorders as well as in β-adrenergic receptor signaling (33). Presence

of a C allele at the -31 position of IL-1β gene promoter leads to decreased expression of

the IL-1β gene due to a specific binding of YY1 in lung epithelial cells (34). YY1

positively regulates IL-6 transcription and is a key molecule involved in

the inflammation process of RA (35). Expression of microRNA-10a was decreased in

the fibroblast-like synoviocytes from RA patients compared with osteoarthritis patients,

and the downregulation was triggered by TNF-α and IL-1β in an NF-κB-dependent

manner through promoting the expression of YY1 (36). These data suggest that C/EBPβ

and YY1 are crucial transcription factors in inflammatory condition.

AMTN is expressed by maturation stage ameloblasts and internal basal lamina of JE,

and the localization suggests that AMTN could play an active role in dentogingival

attachment and maintain the integrity of periodontium. Higher levels of gene expression

for AMTN and ODAM were found in the inflamed gingiva from periodontitis patients

(24, 25). IL-1β and TNF-α increased AMTN mRNA and protein levels in GE1 cells (Fig.

1 and 2). We initially located the IL-1β and TNF-α response region to the proximal

promoter (-116*AMTN*; -116 to +60) of the mouse AMTN gene (Fig. 3), which

encompasses inverted CCAAT, SRY and C/EBP1 elements (Fig. 4). When we used

longer construct (-238*AMTN*; -238 to +60) which including C/EBP2 and YY1 elements

in the promoter sequence for luciferase assays, IL-1β and TNF-α further increased

luciferase activities (Fig. 3). Transcriptional inductions by IL-1β and TNF-α were

partially abrogated when we introduced 3-bp mutations within the C/EBP1, C/EBP2

and YY1 elements and almost completely inhibited when C/EBP1 and C/EBP2 were

double mutated in -460*AMTN* construct (Fig. 5). The involvement of C/EBP1, C/EBP2

and YY1 elements is further supported by gel shift assays in which nuclear proteins that

formed complexes with C/EBP1, C/EBP2 and YY1 were increased by IL-1β and TNF-α

in GE1 cells (Fig. 7). Results of ChIP assays suggest that IL-1β and TNF-α induced AMTN transcription through C/EBPβ and YY1 targeting C/EBP1, C/EBP2 and YY1 elements in the mouse AMTN gene promoter (Fig. 9). The tyrosine kinase inhibitor HA, the MEK1/2 inhibitor U0126 and the PI3K inhibitor LY294002 abrogated the effects IL-1β and TNF-α on AMTN transcription, suggesting that tyrosine kinase, MEK1/2 and PI3K signaling pathways are crucial for IL-1β and TNF-α effect on AMTN gene transcription.

In the second study, we have demonstrated that AMTN mRNA levels were temporally induced by TGFβ1 for a short time, and down-regulated by TGFβ1-induced Bax expression or Bax overexpression in gingival epithelium cells. TGFβ1 possesses a wide range of biological function, such as suppression of proliferation of gingival epithelium cells (37, 38), early embryogenesis (39) and hematopoiesis (40), apoptosis of gingival epithelium cells, and important mechanism to form junctional epithelium (41). Bax overexpression also apparently induced the apoptosis by independent pathway due to Bax expression. ChIP assays utilizing Bax overexpression with/without treatment of TGFβ1 showed that the removal of Smad3 binding to SBEs in AMTN gene promoter. These results consistent with the decreased AMTN mRNA levels by Bax expression.

In conclusion, we have characterized the mouse AMTN gene promoter which is

necessary for IL-1β and TNF-α induced AMTN gene transcription. This promoter region contains C/EBP1, C/EBP2 and YY1 elements which are essential for the IL-1β and TNF-α response. IL-1β and TNF-α induced AMTN gene transcription was inhibited by tyrosine kinase, MEK1/2 and PI3K inhibitors. Furthermore, C/EBPβ and YY1 transcription factors could be key regulators of IL-1β and TNF-α effect on AMTN gene transcription. Additionally, we have demonstrated that TGFβ1- and Smad3-induced AMTN mRNA levels were inhibited by Bax overexpression. These results suggest that the presence of crosstalk between Smad3 and Bax during progression of apoptosis which involved in an indirect interaction between them. Therefore Smad3 may play an important role in TGFβ1 regulation of AMTN gene expression at the apoptosis phase in gingival epithelium. These elucidation suggested that AMTN may be involved in the defense mechanism of periodontal tissue.

Reference

1. Schroeder HE, Listgarten MA (1997) The gingival tissues: the architecture of periodontal protection. Periodontol 2000 13, 91-120.

2. Bosshardt DD, Lang NP (2005) The junctional epithelium: from health to disease. J Dent Res 84, 9-20.

3. Iwasaki K, Bajenova E, Somogyi-Ganss E et al (2005) Amelotin - a novel secreted, ameloblast-specific protein. J Dent Res 84, 1127-1132.

4. Moffatt P, Smith CE, St-Arnaud R, Simmons D, Wright JT, Nanci A (2006) Cloning of rat amelotin and localization of the protein to the basal lamina of maturation stage ameloblasts and junctional epithelium. Biochem J 399, 37-46

5. Somogyi-Ganss E, Nakayama Y, Iwasaki K et al (2012) Comparative temporospatial expression profiling of murine amelotin protein during amelogenesis. Cells Tissues Organs 195, 535-549

6. Lacruz RS, Nakayama Y, Holcroft J, Nguyen V, Somogyi-Ganss E, Snead ML, White SN, Paine ML, Ganss B (2012) Targeted overexpression of amelotin disrupts the microstructure of dental enamel. PLoS One7, e35200.

7. Nakayama Y, Kobayashi R, Matsui S, Matsumura H, Iwai Y, Noda K, Yamazaki M, Kurita-Ochiai T, Yoshimura A, Shinomura T, Ganss B. Ogata Y (2017) Localization and expression pattern of amelotin, odontogenic ameloblast-associated protein and follicular dendritic cell-secreted protein in the junctional epithelium of inflamed gingiva. Odontology 105, 329-337.

8. Nakayama Y, Holcroft J, Ganss B (2015) Enamel hypomineralization and structural defects in amelotin-deficient mice. J Dent Res 94, 697-705.

9. Nishio C, Wazen R, Kuroda S, Moffatt P, Nanci A. (2010) Expression pattern of odontogenic ameloblast-associated and amelotin during formation and regeneration of the junctional epithelium. Eur Cell Mater 20, 393-402.

10. Abbarin N, San Miguel S, Holcroft J, Iwasaki K, Ganss B (2015) The enamel protein amelotin is a promoter of hydroxyapatite mineralization. J Bone Miner Res 30, 775-785.

11. Pihlstrom BL, Michalowicz BS, Johnson NW (2005) Periodontal diseases. Lancet 366, 1809-1820.

12. Kato A, Imai K, Ochiai K, Ogata Y (2013) Higher prevalence of Epstein-Barr virus DNA in deeper periodontal pockets of chronic periodontitis in Japanese patients. PLoS One 8, e71990.

13. Seymour GJ, Gemmell E, Reinhardt RA, Eastcott J, Taubman MA (1993) Immunopathogenesis of chronic inflammatory periodontal disease: cellular and molecular mechanisms. J Periodontal Res 28, 478-486.

14. Netea MG, van Deuren M, Kullberg BJ, Cavaillon JM, Van der Meer JW (2002) Does the shape of lipid A determine the interaction of LPS with Toll-like receptors? Trends Immunol 23, 135-139.

15. Faizuddin M, Bharathi SH, Rohini NV (2003) Estimation of interleukin-1beta levels in the gingival crevicular fluid in health and in inflammatory periodontal disease. J Periodontal Res 38, 111-114.

16. Oh H, Hirano J, Takai H, Ogata Y (2015) Effects of periodontal initial therapy on interleukin-1β levels in gingival crevicular fluid and clinical periodontal parameters. J Oral Sci 57, 67-71.

17. Samoto H, Shimizu E, Matsuda-Honjo Y, Saito R, Yamazaki M, Kasai K, Furuyama S, Sugiya H, Sodek J, Ogata Y (2002) TNF-α Suppresses Bone Sialoprotein (BSP) Expression in ROS17/2.8 Cells. Journal of Cellular Biochemistry 87, 313-323.

18. Yoshimoto T, Fujita T, Kajiya M, Matsuda S, Ouhara K, Shiba H, Kurihara H (2015) Involvement of smad2 and Erk/Akt cascade in TGF-β1-induced apoptosis in human gingival epithelial cells. Cytokine 75, 165-173.

19. Urnowey S, Ansai T, Bitko V, Nakayama K, Takehara T, Barik S (2006) Temporal activation of anti- and pro-apoptotic factors in human gingival fibroblasts infected with the periodontal pathogen, Porphyromonas gingivalis: potential role of bacterial proteases in host signalling. BMC Microbiol 8, 6-26.

20. Alharbi IA, Rouabhia M (2016) Repeated exposure to whole cigarette smoke promotes primary human gingival epithelial cell growth and modulates keratin expression. J Periodontal Res 51, 630-638.

21. Calenic B, Yaegaki K, Kozhuharova A, Imai T (2010) Oral malodorous compound causes oxidative stress and p53-mediated programmed cell death in keratinocyte stem cells. J Periodontol 81, 1317-1323.

22. Fujita T, Alotaibi M, Kitase Y, Kota Y, Ouhara K, Kurihara H, Shuler CF (2012) Smad2 is involved in the apoptosis of murine gingival junctional epithelium associated with inhibition of Bcl-2. Arch Oral Biol 57, 1567-1573.

23. Yoshimoto T, Fujita T, Ouhara K, Kajiya M, Imai H, Shiba H, Kurihara H (2014) Smad2 is involved in Aggregatibacter actinomycetemcomitans-induced apoptosis. J Dent Res 93, 1148-1154.

24. Nakayama Y, Takai H, Matsui S, Matsumura H, Zhou L, Kato A, Ganss B, Ogata Y (2014) Proinflammatory cytokines induce amelotin transcription in human gingival fibroblasts. J Oral Science 56, 261-268.

25. Nakayama Y, Takai H, Matsui S, Zhou L, Abiko Y, Ganss B, Ogata Y (2014) Transcriptional regulation of amelotin gene by proinflammatory cytokines in

gingival fibroblasts. Connect Tissue Res 55, 18-20.

26. Nakayama Y, Matsui S, Noda K, Yamazaki M, Iwai Y, Matsumura H, Izawa T, Tanaka E, Ganss B, Ogata Y (2016) Amelotin gene expression is temporarily being upregulated at the initiation of apoptosis induced by TGFβ1 in mouse gingival epithelial cells. Apoptosis 21, 1057-1070.

27. Ertugrul AS, Sahin H, Dikilitas A, Alpaslan N, Bozoglan A (2013) Comparison of CCL28, interleukin-8, interleukin-1β and tumor necrosis factor-alpha in subjects with gingivitis, chronic periodontitis and generalized aggressive periodontitis. J Periodontal Res 48, 44-51.

28. Ryu OH, Choi SJ, Linares AM, Song IS, Kim YJ, Jang KT, Hart TC (2007) Gingival epithelial cell expression of macrophage inflammatory protein-1alpha induced by interleukin-1beta and lipopolysaccharide. J Periodontol 78, 1627-1634.

29. Fujihara R, Usui M, Yamamoto G, Nishii K, Tsukamoto Y, Okamatsu Y, Sato T, Asou Y, Nakashima K, Yamamoto M. (2014) Tumor necrosis factor-α enhances RANKL expression in gingival epithelial cells via protein kinase A signaling. J Periodontal Res 49, 508-517.

30. Ohno T, Yamamoto G, Hayashi JI, Nishida E, Goto H, Sasaki Y, Kikuchi T, Fukuda M, Hasegawa Y, Mogi M, Mitani A (2017) Angiopoietin-like protein 2 regulates

Porphyromonas gingivalis lipopolysaccharide-induced inflammatory response in human gingival epithelial cells. PLoS One 12, e0184825.

31. Cappello C, Zwergal A, Kanclerski S, Haas SC, Kandemir JD, Huber R, Page S, Brand K (2009) C/EBPbeta enhances NF-kappaB-associated signalling by reducing the level of IkappaB-alpha. Cell Signal 21, 1918-1924.

32. Kim ES, Cha Y, Ham M, Jung J, Kim SG, Hwang S, Kleemann R, Moon A (2014) Inflammatory lipid sphingosine-1-phosphate upregulates C-reactive protein via C/EBPβ and potentiates breast cancer progression. Oncogene 33, 3583-3593.

33. Roos AB, Barton JL, Miller-Larsson A, Dahlberg B, Berg T, Didon L, Nord M (2012) Lung epithelial-C/EBPβ contributes to LPS-induced inflammation and its suppression by formoterol. Biochem Biophys Res Commun 423, 134-139.

34. Landvik NE, Tekpli X, Anmarkrud KH, Haugen A, Zienolddiny S (2012) Molecular characterization of a cancer-related single nucleotide polymorphism in the pro-inflammatory interleukin-1B gene. Mol Carcinog 51 Suppl 1, E168-175.

35. Lin J, He Y, Chen J, Zeng Z, Yang B, Ou Q (2016) Datasets of YY1 expression in rheumatoid arthritis patients. Data in Brief 9, 1034-1038.

36. Mu N, Gu J, Huang T, Zhang C, Shu Z, Li M, Hao Q, Li W, Zhang W, Zhao J, Zhang Y, Huang L, Wang S, Jin X, Xue X, Zhang W, Zhang Y (2016) A novel

NF-κB/YY1/microRNA-10a regulatory circuit in fibroblast-like synoviocytes.

37. Dennison DK, Vallone DR, Pinero GJ, Rittman B, Caffesse RG (1994) Differential effect of TGF-beta 1 and PDGF on proliferation of periodontal ligament cells and gingival fibroblasts. J Periodontol 65, 641-648.

38. de Andrade CR, Cotrin P, Graner E, Almeida OP, Sauk JJ, Coletta RD (2001) Transforming growth factor-beta1 autocrine stimulation regulates fibroblast proliferation in hereditary gingival fibromatosis. J Periodontol 72, 1726-1733.

39. Fang L, Wang YN, Cui XL, Fang SY, Ge JY, Sun Y, Liu ZH (2012) The role and mechanism of action of activin A in neurite outgrowth of chicken embryonic dorsal root ganglia. J Cell Sci 125, 1500–1507.

40. Porowski D, Wirkowska A, Hryniewiecka E, Wyzgał J, Pacholczyk M, Pączek L (2015) Liver failure impairs the intrahepatic elimination of interleukin-6, tumor necrosis factor-alpha, hepatocyte growth factor, and transforming growth factor-beta. Biomed Res Int 934065.

41. Lu H, Mackenzie IC, Levine AE (1997) Transforming growth factor-beta response and expression in junctional and oral gingival epithelial cells. J Periodontal Res 32, 682-691.
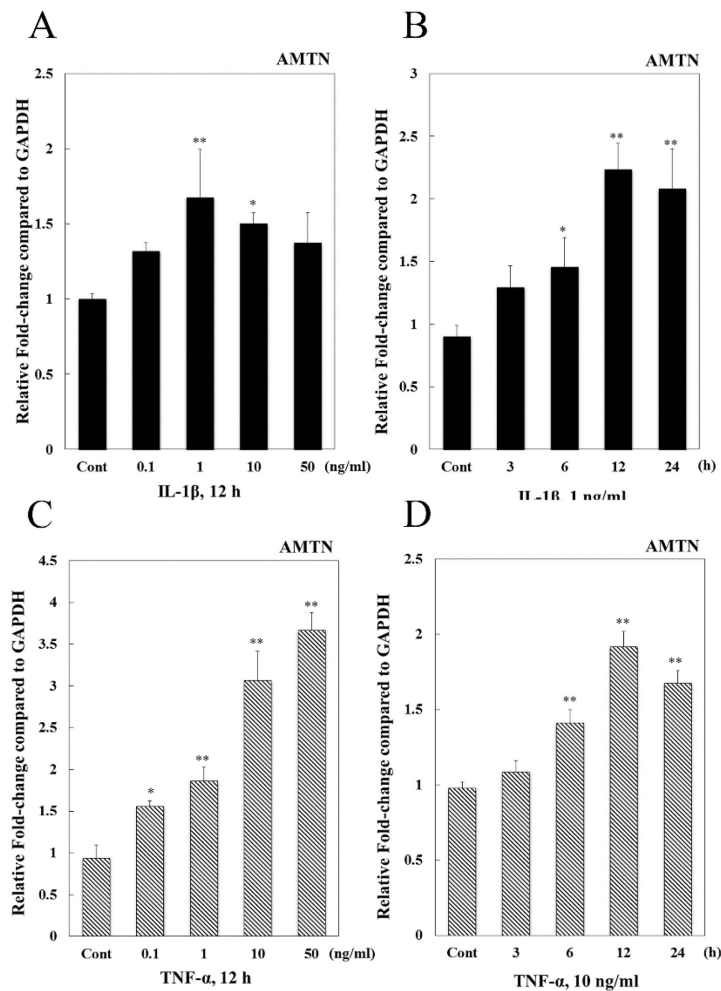
Fig. 1 Effects of IL-1β and TNF-α on AMTN mRNA expressions in mouse gingival epithelial GE1 cells. (A) Dose-response effects of IL-1β (0.1, 1, 10, 50 ng/ml) on AMTN mRNA levels in GE1 cells treated for 12 h. (B) GE1 cells were treated with or without IL-1β (1 ng/ml) for 3, 6, 12, and 24 h. (C) Dose-response effects of TNF-α (0.1, 1, 10, 50 ng/ml) on AMTN mRNA levels in GE1 cells treated for 12 h. (D) GE1 cells were treated with or without TNF-α (10 ng/ml) for 3, 6, 12, and 24 h. The expressions of AMTN and GAPDH mRNA in GE1 cells were measured by real-time PCR. The experiments were performed in triplicate for each data point. Quantitative analyses of the data sets are shown with standard errors (SE). Significantly different from control, *$P < 0.05$, **$P < 0.01$.

36
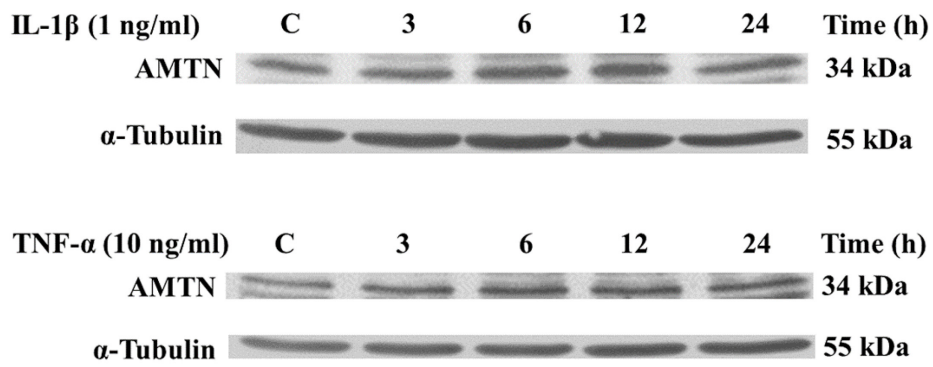
Fig. 2 The expression of AMTN protein in GE1 cells was analyzed by Western blotting using an anti-AMTN antibody. Anti-α tubulin antibody was used as a loading control.
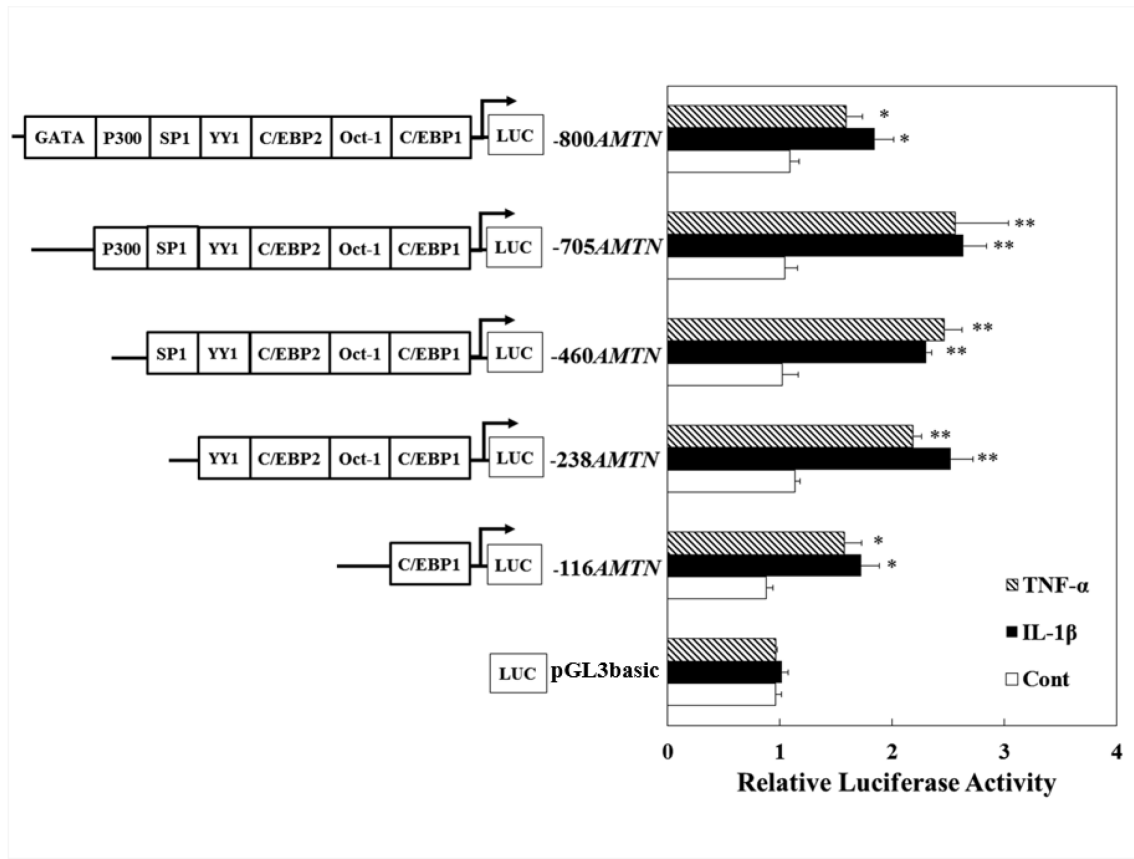
Fig. 3 IL-1β and TNF-α upregulates mouse AMTN promoter activities. Transcriptional activities of -116*AMTN*, -238*AMTN*, -460*AMTN*, -705*AMTN* and -800*AMTN* were increased after 12 h treatment with IL-1β (1 ng/ml) and TNF-α (10 ng/ml) in GE1 cells. The transcriptional activities determined from three separate transfections with constructs, pGL3 basic and -116*AMTN* to -800*AMTN*, have been combined, and the values expressed with SE. Significant differences from control: *$P < 0.05$, **$P < 0.01$.
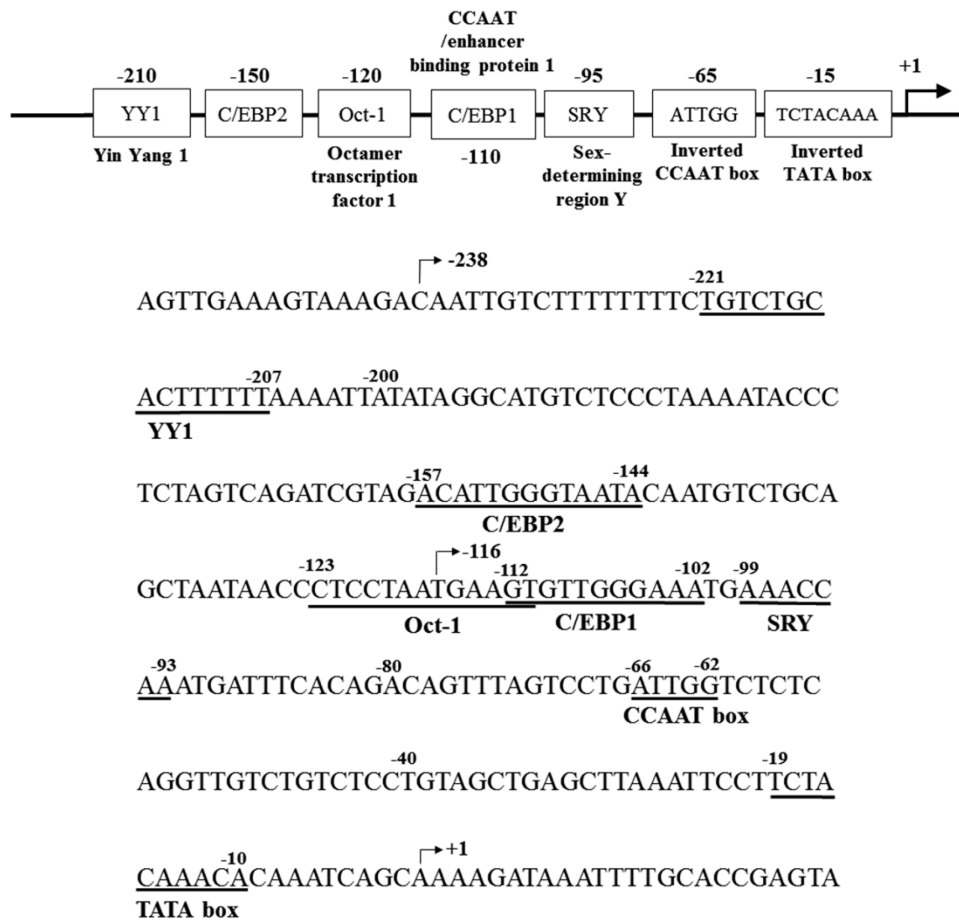
Fig. 4 Regulatory elements in the proximal promoter of the mouse AMTN gene. **Upper panel:** The positions of inverted TATA and CCAAT boxes, SRY, C/EBP1, Oct-1, C/EBP2, and YY1 are shown. The numbering of nucleotides is relative to the transcription start site (+1). **Lower panel:** Nucleotide sequences of the mouse AMTN gene proximal promoter is shown from -253 to +24. An inverted TATA box, inverted CCAAT box, SRY, C/EBP1, Oct-1, C/EBP2 and YY1 are present.
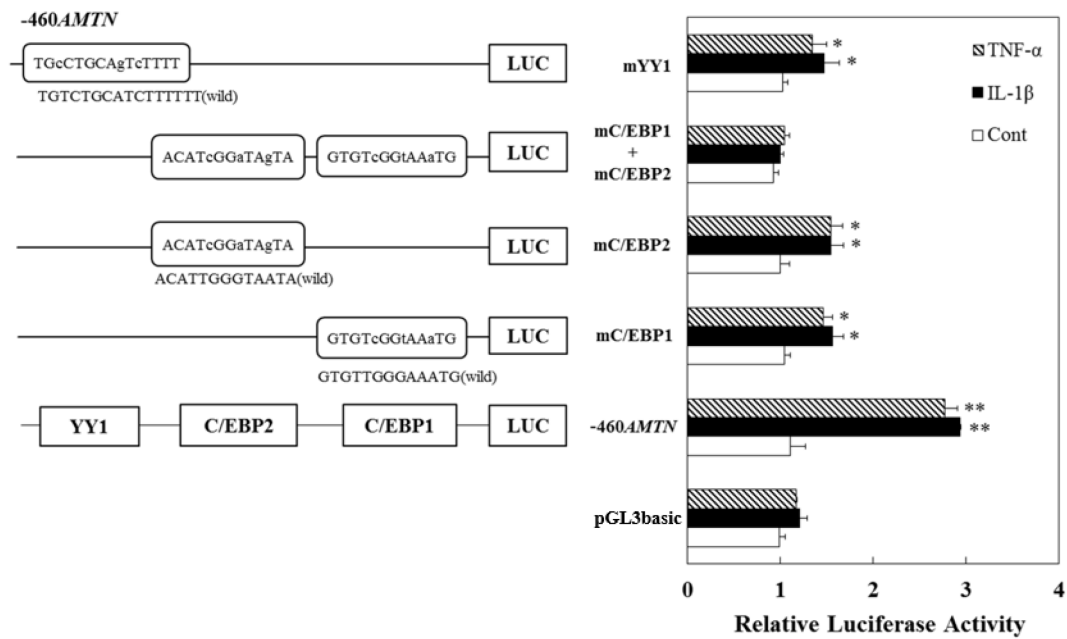
Fig. 5 Site-specific mutation analyses of luciferase activities. After introducing 3-bp mutations, transcriptional induction by IL-1β and TNF-α was partially inhibited in the mC/EBP1, mC/EBP2 and mYY1. Double mutation in C/EBP1 and C/EBP2 (mC/EBP1 + mC/EBP2) completely abolished the effect of IL-1β and TNF-α. The results of transcriptional activities obtained from three separate transfections with constructs were combined and values expressed with SE. Significantly different from control, *$P < 0.05$, **$P < 0.01$.
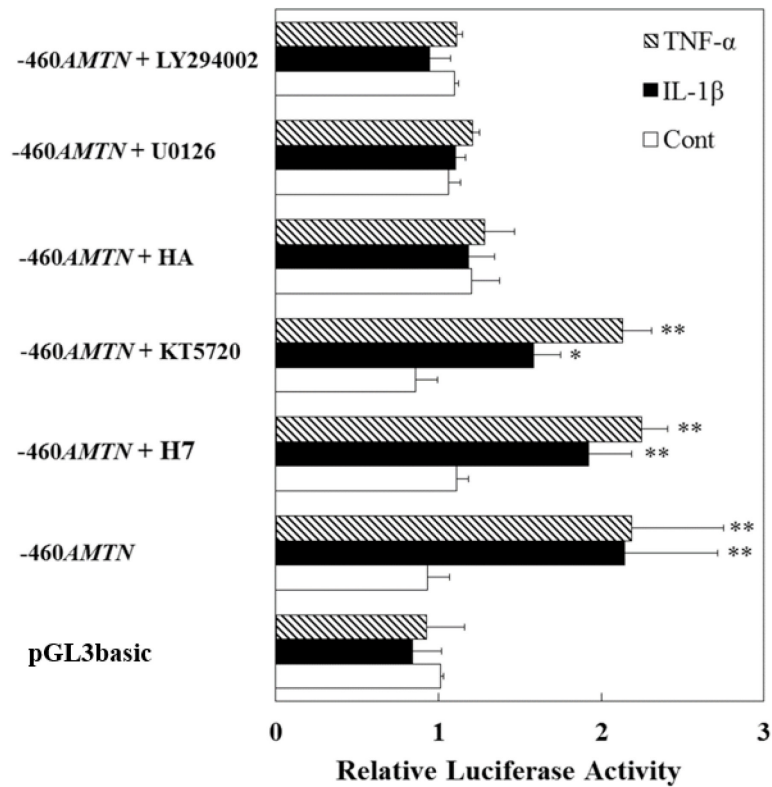
Fig. 6 Effects of kinase inhibitors on transcriptional activation by IL-1β and TNF-α. IL-1β (1 ng/ml) and TNF-α (10 ng/ml) induced -460*AMTN* activation was inhibited by tyrosine kinase (HA), ERK 1/2 (U0126) and PI3K (LY294002) inhibitors, and no effects were observed for PKC (H7) and PKA (KT5720) inhibitors. The results of transcriptional activities obtained from three separate transfections with constructs were combined and the values were expressed with SE. Significant differences from control: *$P < 0.05$, **$P < 0.01$.
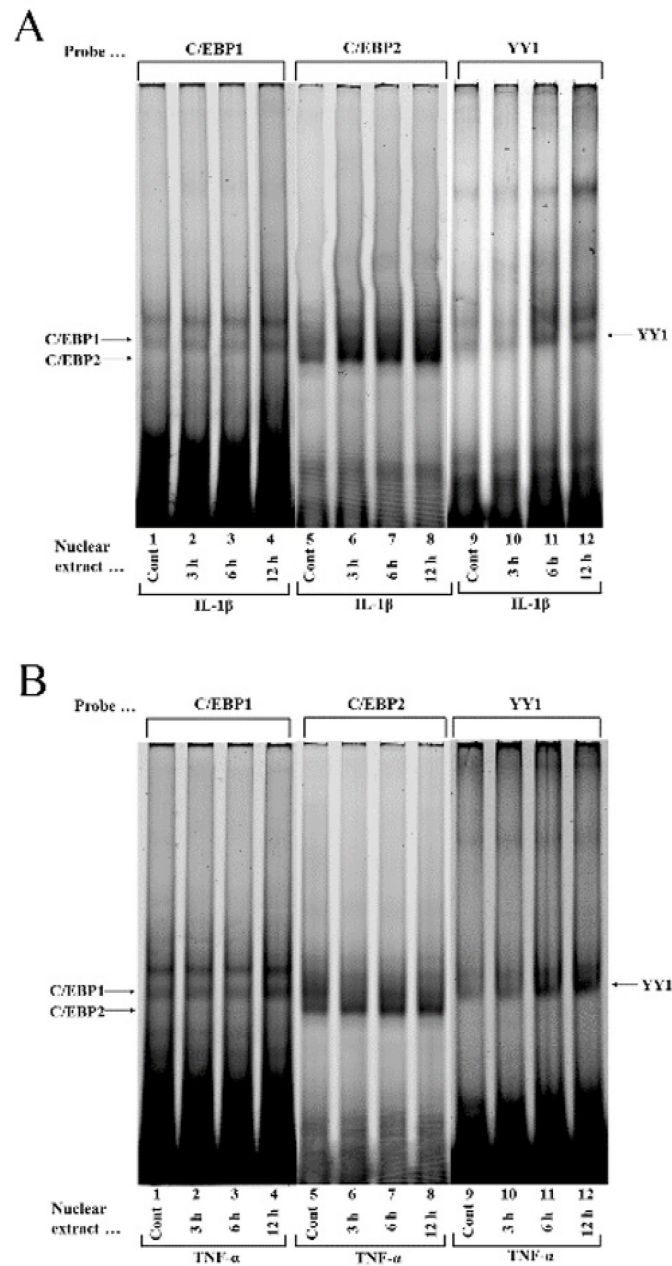
Fig. 7 Gel mobility shift assays using C/EBP1, C/EBP2 and YY1. After stimulation by IL-1β (1 ng/ml; 3, 6 and 12 h) or TNF-α (10 ng/ml; 3, 6, and 12 h), C/EBP1–protein complex was increased at 12 h (lanes 1-4), C/EBP2–protein complex was increased at 3, 6 and 12 h (lanes 5-8), YY1–protein complex was increased at 6 h and 12 h (lanes 9-12). DNA-protein complexes were separated in a 6 % polyacrylamide gel with a low ionic strength Tris-borate buffer, and quantitation using an imaging analyzer.
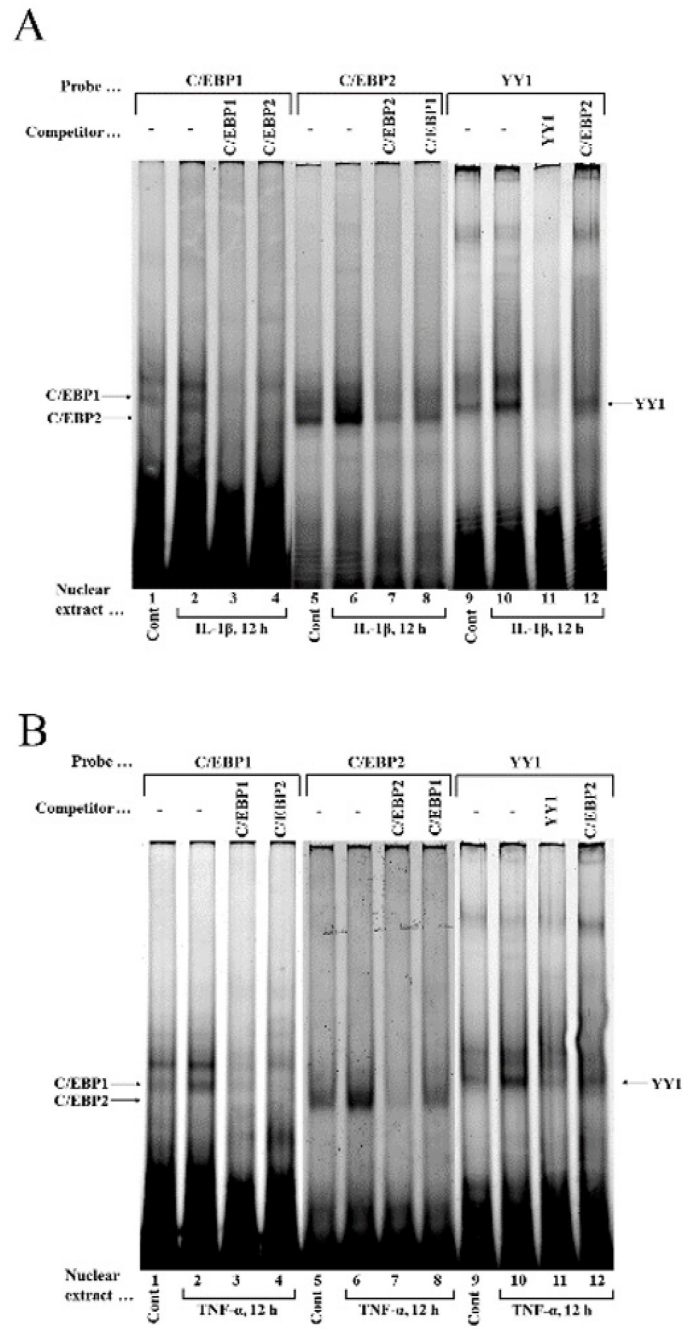
Fig. 8 Specific binding of nuclear proteins to C/EBP1, C/EBP2 and YY1. A 40-fold molar excess of C/EBP1, C/EBP2 and YY1 reduced DNA-protein complexes formation (lanes 3, 4, 7, 8, 11 and 12).
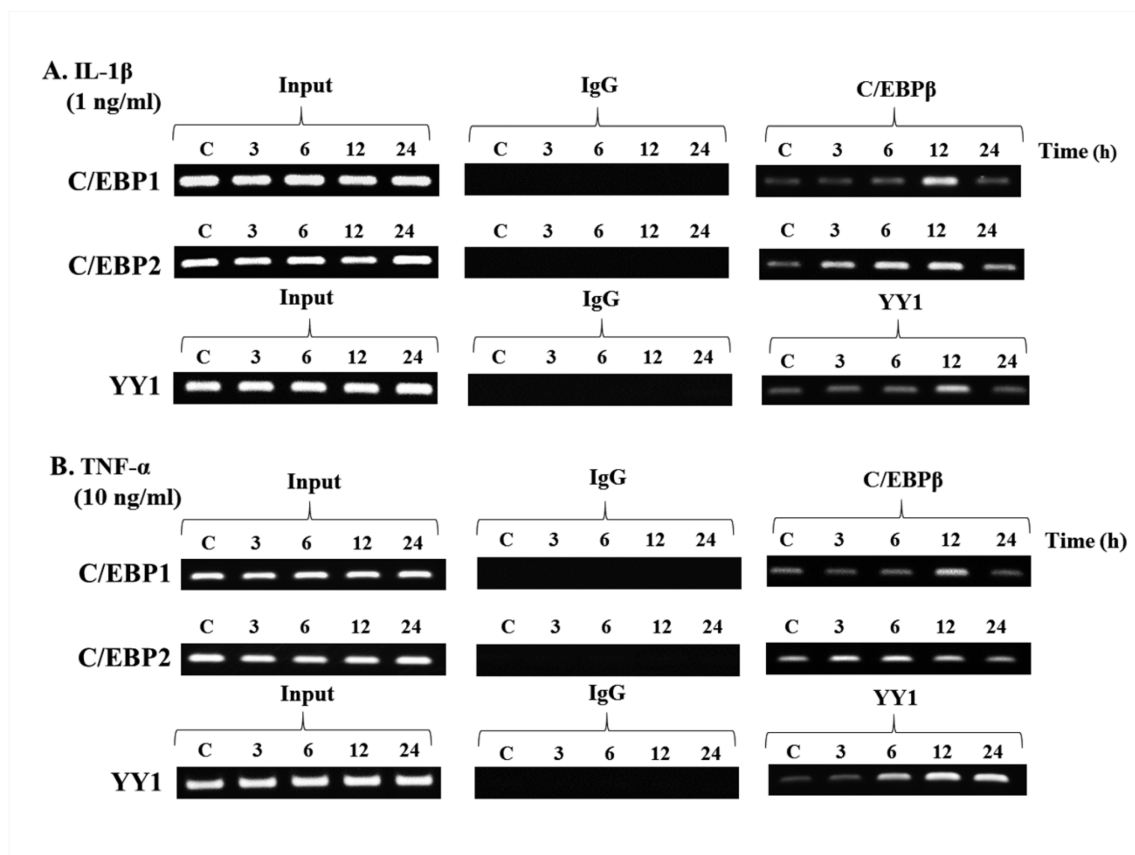
Fig. 9 ChIP analyses of transcription factors binding to C/EBP1, C/EBP2 and YY1 sites in the mouse AMTN promoter in GE1 cells. The PCR bands amplified and corresponding to DNA-protein complexes immunoprecipitated with antibody revealed that C/EBPβ interacted with a chromatin fragment containing the C/EBP1 and C/EBP2 were increased in GE1 cells. YY1 interacted with a chromatin fragment containing the YY1 was increased in GE1 cells after stimulation by IL-1β (1 ng/ml) and TNF-α (10 ng/ml).
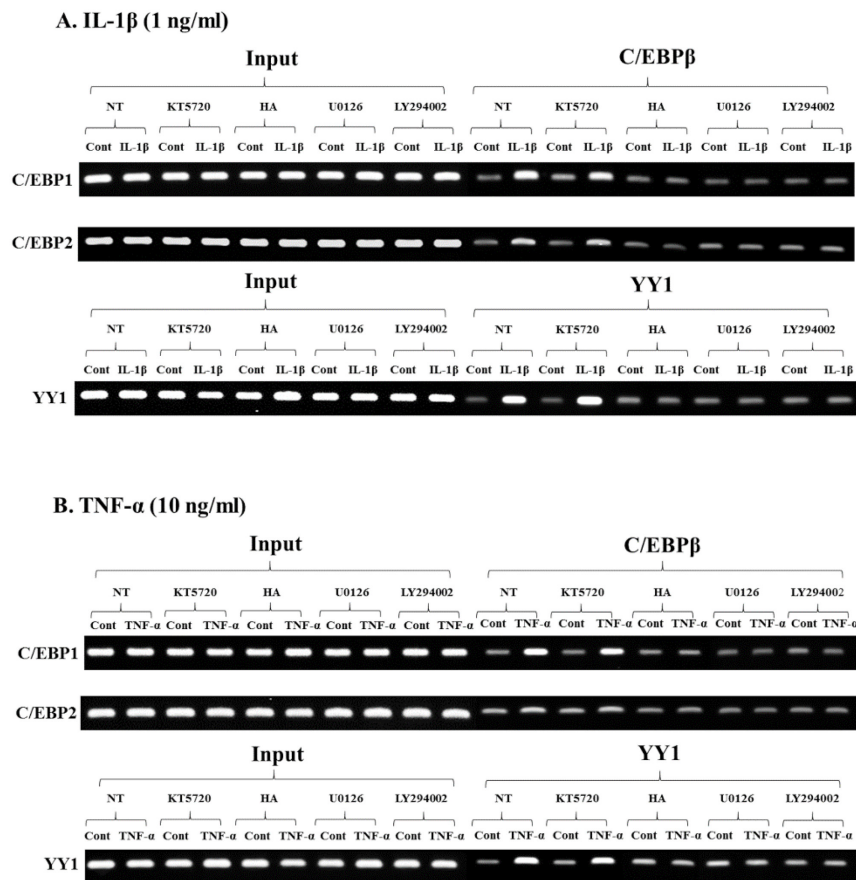
Fig. 10 Effects of kinase inhibitors on DNA-protein complex formations after IL-1β and TNF-stimulation. ChIP assays were performed using various kinase inhibitors. C/EBPβ binding to the C/EBP1 and C/EBP2, and YY1 binding to YY1 were inhibited by HA, U0126 and LY294002, but not inhibited by H7 and KT5720.
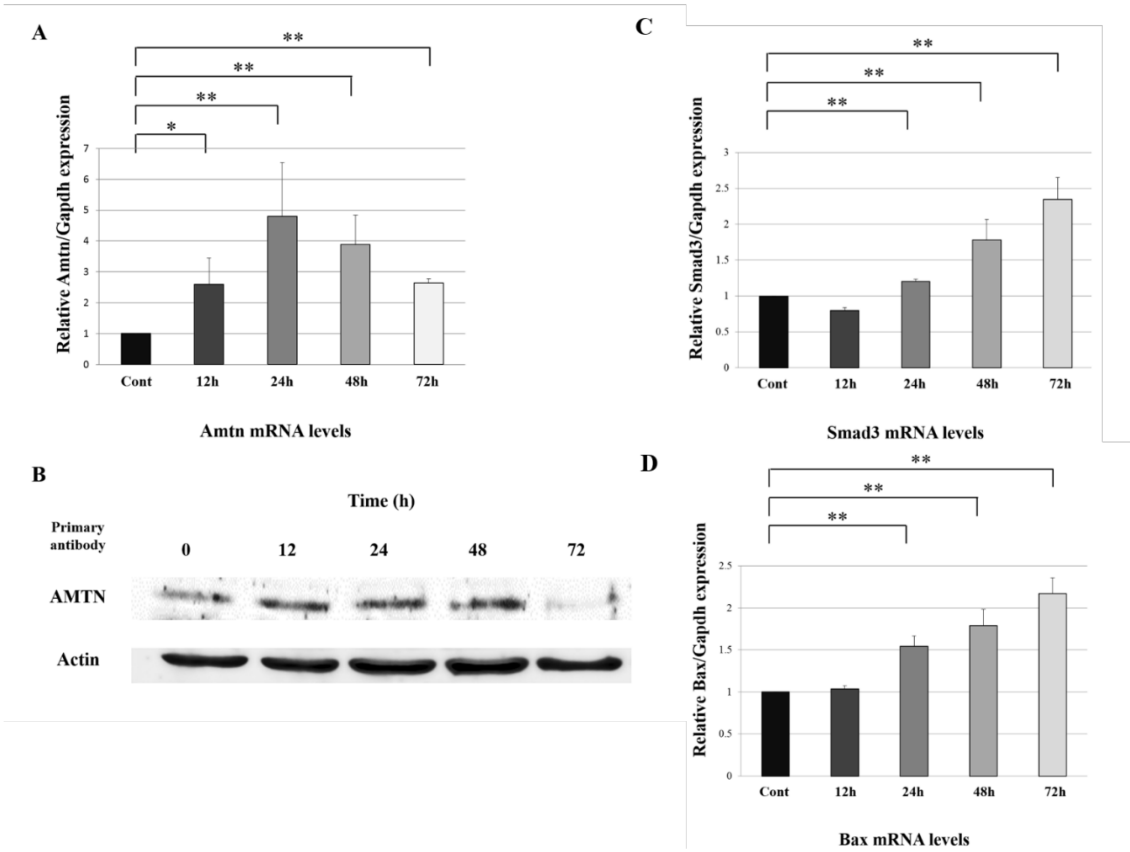
Fig. 11 AMTN mRNA levels were temporally induced by TGFβ1 in GE1 cells. (A) AMTN mRNA levels were increased by TGFβ1 (10 ng/ml) treatment and reached maximal at 24 h, then immediately decreased. (B) AMTN protein expression increased in agreement with the change of their mRNA levels. (C, D) Smad3 and Bax mRNA levels were upregulated by TGFβ1 (10 ng/ml) in GE1 cells. Significant differences from control: *$P < 0.05$, **$P < 0.01$.
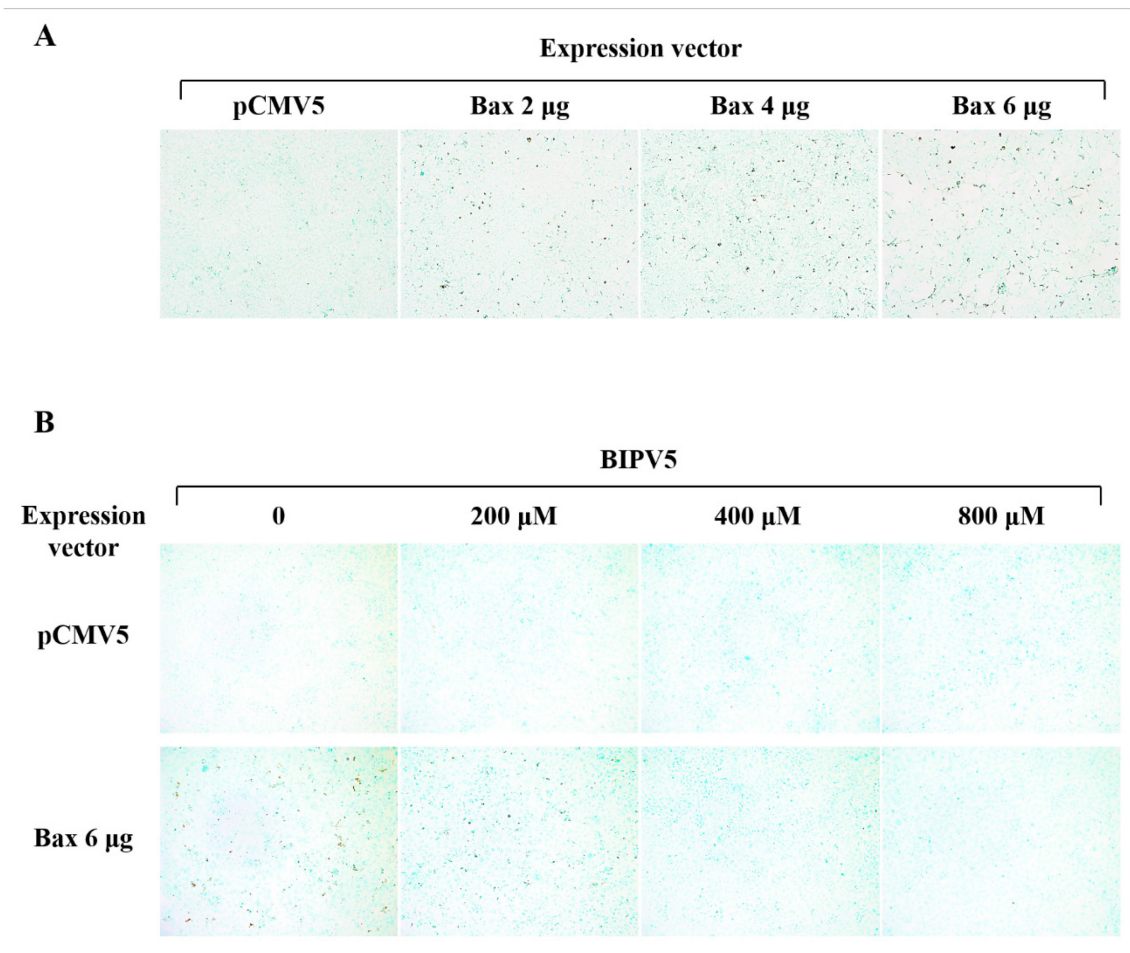
Fig. 12 Bax overexpression induced apoptosis in GE1 cells. (A) Apoptosis *in situ* detection was evaluated by overexpression of Bax (2, 4 and 6 μg) by using TUNEL staining, Bax overexpressions induced apoptosis in dose dependent. Cell detachment was partialy detected by overexpression of Bax (6 μg). (B) The addition of dose dependent BIPV5 peptide resulted in the repression of apoptosis induced by Bax overexpression (6 μg).
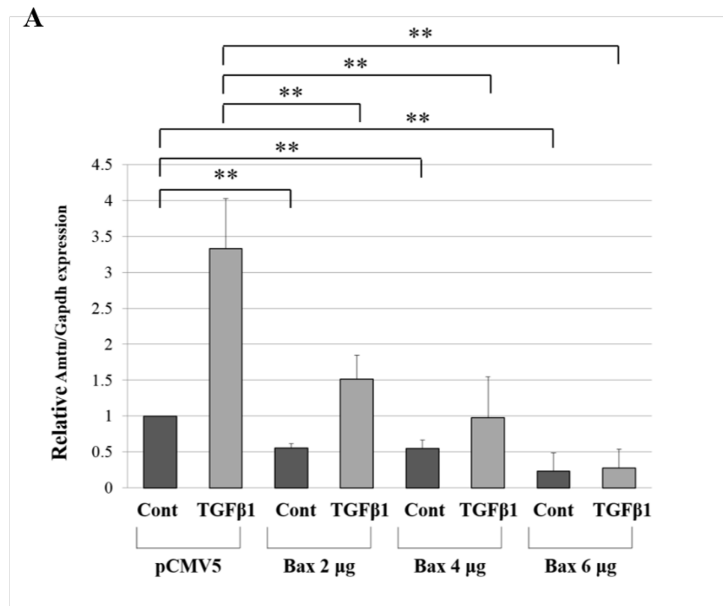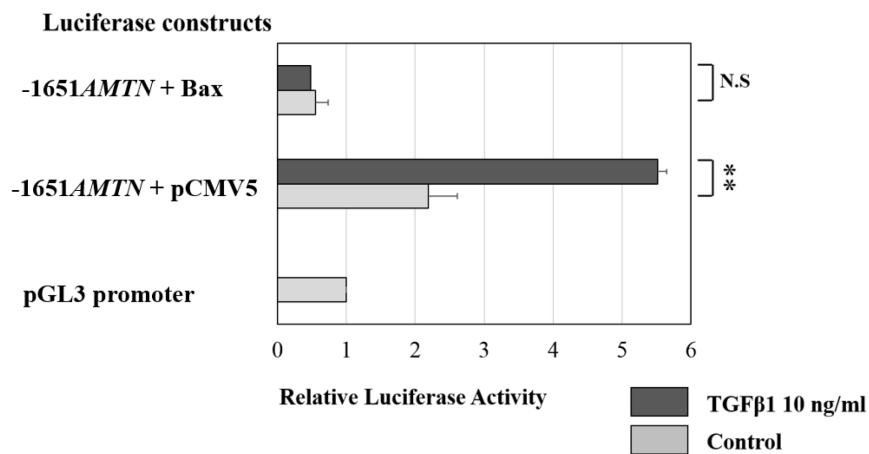
Fig. 13 (A) AMTN gene expression induced by TGFβ1 (10 ng/ml) were down-regulated by the dose dependent overexpression of Bax in GE1 cells. Not only AMTN mRNA levels induced by treatment of TGFβ1, but also controls were inhibited by dose dependent overexpression of Bax. (B) Luciferase activities of -1651AMTN constructs (-1651 to +60) were significantly increased by TGFβ1 (10 ng/ml, 24 h). Basal and TGFβ1 induced luciferase activities were inhibited by Bax overexpression (6 μg). Significant differences from control: *$P < 0.05$, **$P < 0.01$.
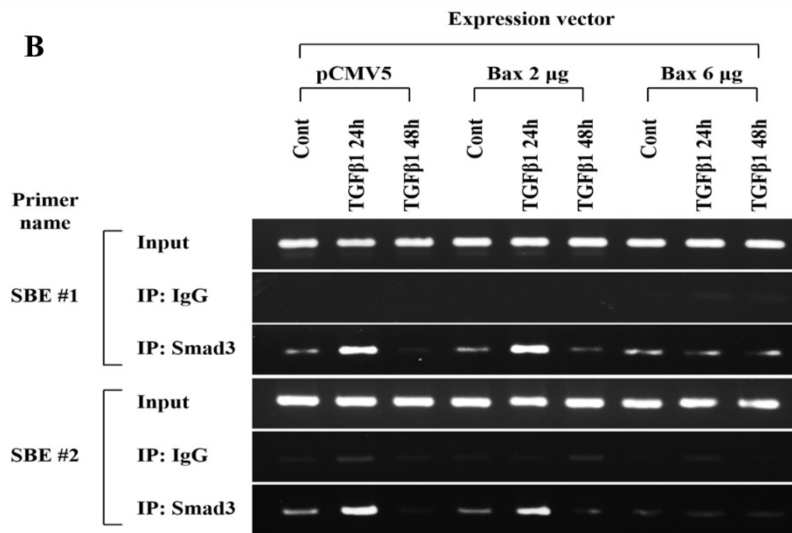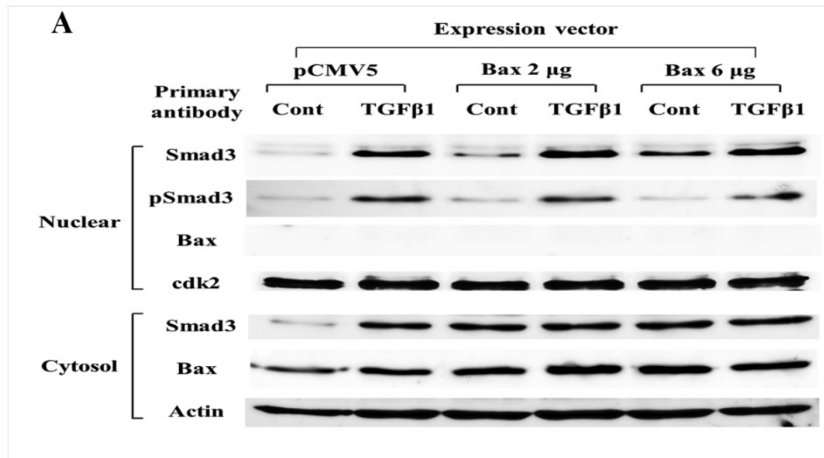
Fig. 14 Smad3 bindings to SBEs were blocked by Bax overexpression in GE1 cells. (A) Smad3 and pSmad3 expression that induced by TGFβ1 (10 ng/ml, 24 h) were not inhibited by overexpression of Bax (2 and 6 μg) in nuclear extracts and cytosol in GE1 cells. Cdk2 and Actin expressions were not changed by 24 h treatment of TGFβ1 and overexpression of Bax. And also overexpression of Bax in cytosol were confirmed. (B) Smad3 bindings to SBE#1 and #2 were increased by TGFβ1 (10 ng/ml) at 24 h and decreased at 48 h in expression of pCMV5 control plasmids. Smad3 bindings to SBE#1 and #2 induced by TGFβ1 were inhibited almost completely by Bax (6 μg) overexpression, but not by Bax (2 μg).